

TURBINE BLADE FRICTION DAMPING STUDY

Robert J. Dominic
University of Dayton Research Institute
Dayton, Ohio 45469

Abstract

An analytical and test evaluation were conducted to determine the performance of turbine blade platform friction dampers used to control the lower order flexural modes of a blade. The configuration used in the study was the first stage turbine of the high pressure fuel turbopump (HPFTP) of the space shuttle main engine (SSME). The analytical study used the lumped parameter method developed by Jones and Muszynska¹ as implemented on a VAX 11/780 computer. It showed that the primary parameters affecting the friction damper performance are: the damper-blade coefficient of friction; the normal force applied to the friction interface; the amplitude of the periodic forcing function; the relative phase angle of the forcing functions for adjacent blades bridged by a damper (effectively, the engine order of the forcing function); and the amount of hysteretic damping that acts to limit the vibration amplitude of the blade in its resonance modes. In addition, the analytical study showed that overdamping of the blade, resulting in fixity at the platform and a consequent lightly-damped flexural resonance mode of the blade airfoil section alone, is likely to occur in a high-speed turbine such as the HPFTP because of the high normal force applied to the friction interface by the centrifugal force acting on the damper. A test study was performed in a high speed spin pit to evaluate the low order flexural resonance vibration modes of HPFTP blades without dampers, with production dampers, and with two types of lightweight experimental dampers. The test program results agreed with the results of the analytical study in that blades fitted with production friction dampers experienced the airfoil-alone flexural resonance mode, while those without dampers or with lighter weight dampers did not. Likewise, no blades

fitted with dampers experienced the whole blade flexural resonance mode during high speed tests, while those without dampers did.

Background

Three catastrophic failures of HPFTP first stage turbine blades occurred during test stand runs early in the SSME development program. These failures were attributed to lockup of the platforms of adjacent blades, in one case due to welding of the underplatform friction dampers to the platforms because of overtemperature conditions during the run, in another case due to extrusion of a nickelplate antifriction coating on the dampers into the interplatform gap, and in a third case due to an out of tolerance build that reduced or eliminated the interplatform gap for some blades in the stage. The mechanism of the failures was determined to be high cycle fatigue caused by excessive vibration of the blades. Failures occurred near the base of the airfoil section of the blades, just above the platform. Figure 1 shows two of the subject blades and the friction dampers that are placed in slots below the platforms and act on the bottom surface of the platforms to reduce the flexural vibrations of the blades through the absorption of energy by friction heating.

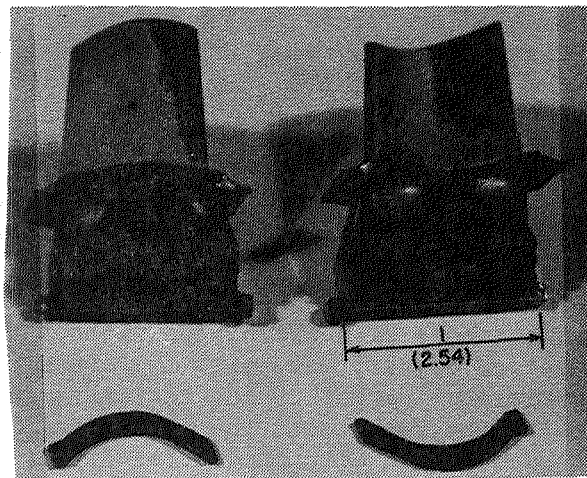


FIG. 1 HPFTP 1st STAGE BLADES AND DAMPERS

During pump operation the dampers also act to limit the leakage of cooling hydrogen, which is routed over the blade roots, into the turbine drive fluid stream. The dampers are forced against the under surface of the platforms by a combination of centrifugal force and the differential pressure between the cooling hydrogen and the turbine drive fluid.

The 63 blade turbine wheel is fed by 41 first stage nozzles. Thirteen shaft front bearing support struts are aligned with 13 of the nozzles in a necessarily unsymmetrical arrangement with 11 struts aligned three nozzles apart and two struts aligned four nozzles apart. Pressure pulses caused by the wakes off the nozzles, and particularly the higher amplitude pulses for the nozzles aligned with struts, excite vibrations in the blades that cause the high cycle fatigue problems. The repetition frequencies for these pulses are $10\frac{1}{4}$ per rev for struts spaced four nozzles apart, $13\frac{2}{3}$ per rev for struts spaced three nozzles apart, and 41 per rev for the symmetrically spaced nozzles. Sum and difference frequencies of these excitation components and their harmonics occur also to provide wide band excitation of the blades. The $13\frac{2}{3}$ per rev (14E) excitation of the blades is shown later to be a critical excitation frequency in the operating regime of the blades.

The nature of the blade fatigue failures caused them to be attributed to flexural resonance modes of the blades. Modal studies of the blades showed that the first two bending modes of the blade occurred at approximately 4,500 and 18,000 Hz. Later, during a whirligig spin test program² conducted by Rocketdyne, a resonance condition near 8,500 Hz was found. This resonance condition was first described as the first torsional mode of the blade (which actually occurs at approximately 11,000 Hz), but it was later identified by the University of Dayton Research Institute (UDRI) as the first flexural mode of the airfoil section of the blade when the platforms are constrained from motion. The 14E excitation pulses occur at this airfoil-alone flexural resonance frequency of the

blades during the long (relatively) time periods of engine operation at RPL.

As a result of the early studies the strut contour was changed to reduce the energy in the excitation pulses and the platform friction damper weight was reduced to provide more optimum damping. However, fatigue cracking continued to occur near the airfoil root with the platform at much lower than the specified and predicted life for the blades. Subsequently, UDRI contracted with NASA to evaluate the operation of the blade-damper system analytically, using the lumped parameter analysis, and to evaluate the operation of a test system in a high speed spin pit.

Analytical Study Using the Lumped Parameter (Lumped Mass) Analysis

The lumped mass analysis used evaluates a blade only in its lower order flexural modes and only for the steady state solution. The blade is represented by two concentrated masses (m_1, m_2) supported in series by two flexural springs (k_1, k_2) with a hysteretic loss factor (η_1, η_2) associated with each spring. The hysteretic loss factors represent the combination of root damping, aerodynamic damping, and material damping in the operating blade. The concentrated masses and flexural springs represent the modal parameters of the blade in the flexural plane. The modal parameters for the SSME HPFTP first stage blade can be determined from the resonance equations of the blade in three flexural resonance conditions, as shown in Figure 2. The resonance frequencies f_1, f_2, f_3 have been measured in test programs as follows: f_1 has been measured by Rocketdyne Division of Rockwell International (RDRI) in siren tests and by UDRI in impact tests; f_2 has been measured by (RDRI) in siren tests; f_3 was shown in the (RDRI) whirligig test data² on blades with welded platforms and on blades with friction dampers when the dampers greatly limited platform motion. These values are average values for several blades.

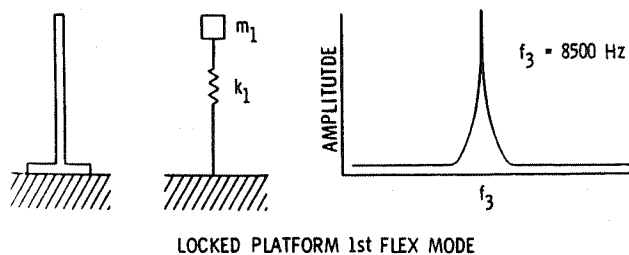
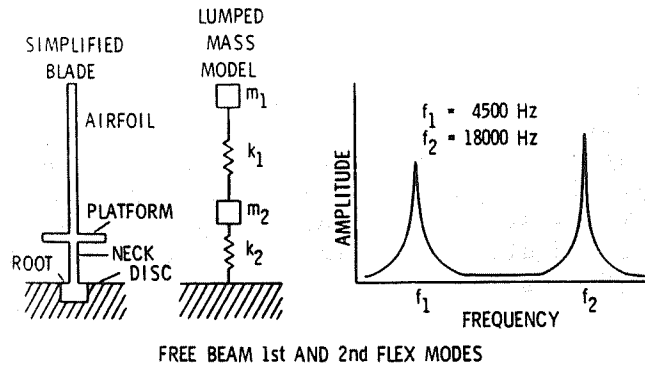


FIG. 2 HPFTP 1st STAGE BLADE FLEX MODES

Three resonance equations can be derived, two for the free blade and one for the platform locked blade, as below.

$$\frac{k_1 k_2}{m_1 m_2} = (4\pi^2 f_1 f_2)^2 \tag{1}$$

$$\frac{k_1 + k_2}{m_2} + \frac{k_1}{m_1} = 4\pi^2 (f_1^2 + f_2^2) \tag{2}$$

$$\frac{k_1}{m_1} = (2\pi f_3)^2 \tag{3}$$

These three equations can be simplified algebraically to state three of the unknown parameters in terms of the fourth. Then if one is assigned a value the other three parameters are defined. Any consistent set of units can be used. We assigned $m_1 = 0.02$ pound, then

$m_2 = 0.007975$ pound, $k_1 = 5.705 \times 10^7$ pounds/inch, and $k_2 = 2.859 \times 10^7$ pounds/inch.

If a series of these blades are installed in a rigid disk with platform friction dampers between the blades and with airfoil excitation forces imposed, the discrete bladed disk model shown in Figure 3 is evolved. This system is a modal analog of the HPFTP first stage bladed disk in the frequency range of 0 to perhaps 20,000 Hz.

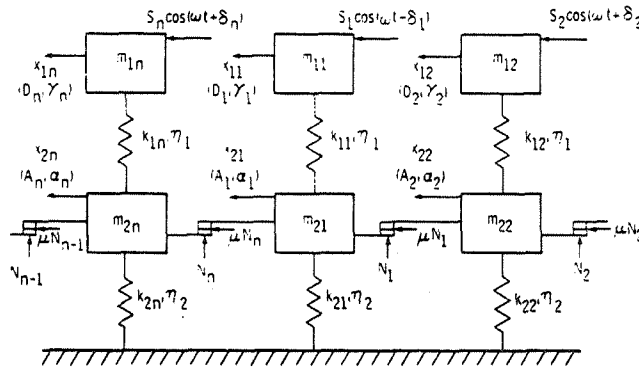


FIG. 3 LUMPED MASS MODEL OF BLADED DISK SYSTEM

The equations of motion for the v th blade in Figure 3 are:

$$m_{1v} \ddot{x}_{1v} + k_{1v} (x_{1v} - x_{2v}) + \frac{k_{1v} \eta_1}{\omega} (\dot{x}_{1v} - \dot{x}_{2v}) = S_v \cos(\omega t + \delta_v) \quad (4)$$

$$m_{2v} \ddot{x}_{2v} - k_{1v} x_{1v} + \frac{k_{1v} \eta_1}{\omega} (\dot{x}_{2v} - \dot{x}_{1v}) + \frac{k_{2v} \eta_2}{\omega} \dot{x}_{2v} + \mu N_v \text{sign}$$

$$(\dot{x}_{2v} - \dot{x}_{2,v+1}) + \mu N_{v-1} \text{sign}(\dot{x}_{2v} - \dot{x}_{2,v-1}) + (k_{1v} + k_{2v}) x_{2v} = 0 \quad (5)$$

for $v = 1, 2, \dots, n$, where n is the number of blades in the system. These are a set of nonlinear equations of the second order, the only nonlinear terms representing a Coulomb model of the friction forces on the platform. The previously undefined terms in these equations are the harmonic excitation force, $S_v \cos(\omega t + \delta_v)$, the

coefficient of friction, μ , the normal force on the friction surface, N_v , and the deflections of the modal masses, X_1 and X_2 . The phase angle, δ_v , represents the time lag of a traveling wave excitation around the disk system. This is representative of the spinning blade system passing through pressure disturbances caused by the nozzle vane and shaft front support strut wakes.

This system of equations is solved using the method of harmonic balance. A nonlinear matrix iteration is used to obtain a numerical solution.¹ The solution, obtained by computer, consists of the deflection amplitudes D_v , A_v , and the phase angles γ_v , α_v , for the outboard (airfoil) and inboard (platform and neck) modal masses of each blade as a function of the system parameters m_{1v} , m_{2v} , k_{1v} , k_{2v} , N_v , S_v , δ_v , μ , η_1 , η_2 , and ω . Since most of the system parameters are input to the computer as arrays many types of mistuned systems can be evaluated. Only solutions for a tuned system have been evaluated to date, specifically, a tuned system with the HPFTP average blade.

The usual analysis is a series of computer runs with η_1 , η_2 , μ , and S constant and N varying from 0 to a selected upper limit in steps for successive runs. In each run solutions are obtained from a lower starting frequency to an upper ending frequency at fixed increments of the frequency range. The range from 3,000 to 12,000 Hz has been evaluated in 100 Hz or 250 Hz increments in most runs because failures at the 8,500 Hz mode when platform lockup occurs are of major interest. A few runs from 3,000 to 20,000 Hz have been processed and show that the friction damping is as effective at the second flexural mode of the free blade (18,000 Hz) as it is at the first flexural mode (4,500 Hz).

Another controlling parameter of the friction damper performance is the blade to adjacent blade phasing. One would expect that when adjacent blades are in phase no damping by the interplatform friction dampers would occur. Conversely, maximum damping

would be expected when blades are out of phase. The interblade phase angle is controlled by δ_v , the phase shift of the harmonic forcing function $S \cos(\omega t + \delta_v)$, and is input to each run as an array. The value of δ_v , the phase angle of the v th blade for a phase tuned system is defined as:

$$\delta_v = \frac{2\pi E(v-1)}{n} \quad (6)$$

where E is the engine order of the vibration mode and n is the total number of blades in the disk. The blade to blade phase shift is designated θ , defined as:

$$\theta = \frac{2\pi E}{n} = \delta_v - \delta_{(v-1)} \quad (7)$$

A sample of program output data for the outboard modal mass deflection is presented in Figure 4 as a plot of amplitude D versus frequency and a similar set of data for the inboard modal mass deflection (amplitude A) is presented in Figure 5 for the same computer runs. These data sets arise from runs of the lumped mass program with the N variable successively assigned the values shown in the tables on the figures. The other system parameters for these runs were:

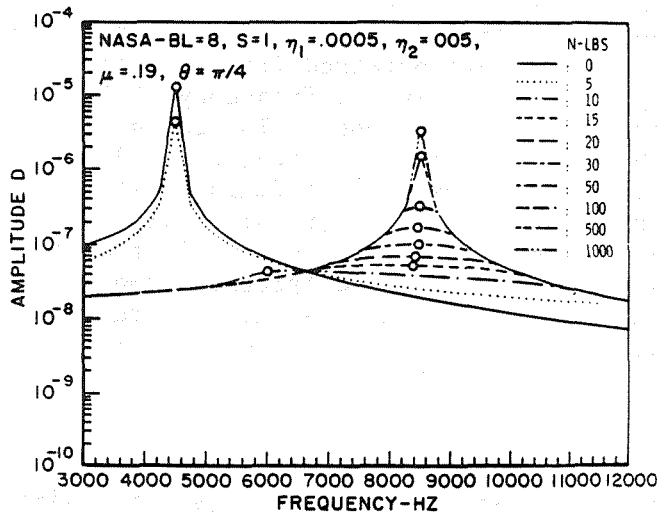


FIG. 4 AMPLITUDE OF HPFTP BLADE MODAL MASS m_1 VERSUS FREQUENCY OF EXCITATION

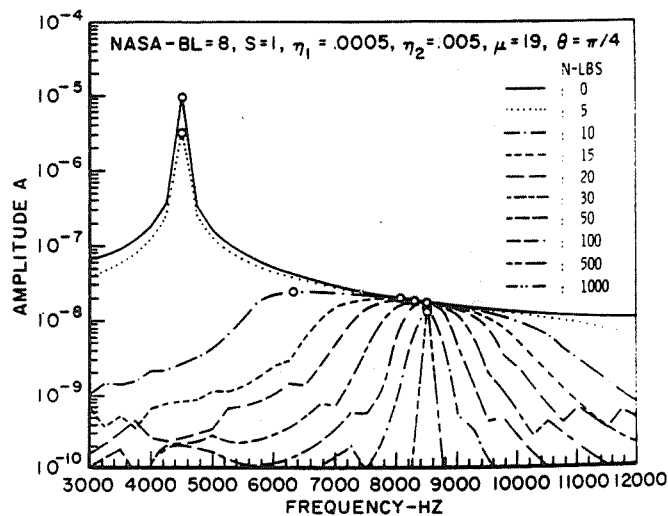


FIG. 5 AMPLITUDE OF HPFTP BLADE MODAL MASS m_2 VERSUS FREQUENCY OF EXCITATION

$$\theta = \pi/4 \text{ (8 bladed disk)}$$

$$S = 1.0 \text{ lb. } \cos(\omega t + \frac{2\pi(\nu-1)}{8})$$

$$\mu = 0.19$$

$$\eta_1 = 0.0005$$

$$\eta_2 = 0.005$$

and m_1, m_2, k_1, k_2 = HPFTP average blade modal values for the tuned first stage disk system. The η_2 value of 0.005 is an average value obtained during modal tests of blades hard-clamped in a broach block. Figures 4 and 5 show that the blade transitions very quickly from the 4,500 Hz mode to the 8,500 Hz mode at low values of N or $\mu N/S$ and that the minimum response of the blade occurs in this transition region near the midfrequency of the region.

Figure 6 shows the plots of the peak amplitude of the airfoil modal mass deflection relative to the platform-neck modal mass deflection ($D-A$) versus the ratio

$\mu N/S$, the ratio of the friction force opposing platform motion to the blade forcing function amplitude.

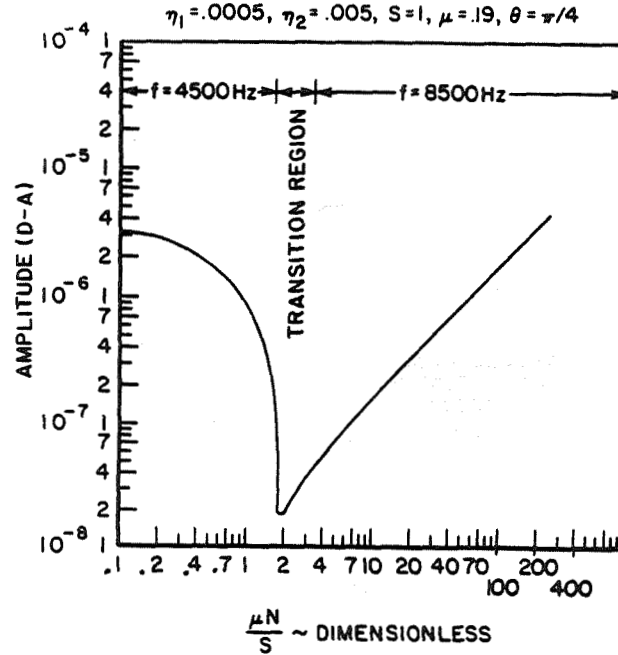


FIG. 6 AMPLITUDE OF m_1 RELATIVE TO m_2 VS $\frac{\mu N}{S}$

The data points selected for the Figure 6 plot are circled on Figures 4 and 5. Figures 4 and 5 show that the blade vibration amplitude is reduced optimally by friction damping at relatively low values of N . This fact is depicted very graphically in Figure 6. The transition region also is shown in Figure 6.

Figure 7 shows the effect of changes in the hysteretic loss factors η_1 and η_2 while all other parameters remain unchanged. Figure 7 shows that hysteretic damping is effective at the 4,500 Hz modal frequency. After the friction damping forces the frequency into the transition region, however, the effect of the hysteretic damping becomes negligible.

Figure 8 shows the effect of variation of θ , the blade to blade phase angle. It is seen that a larger phase shift between blades up to an equivalent engine

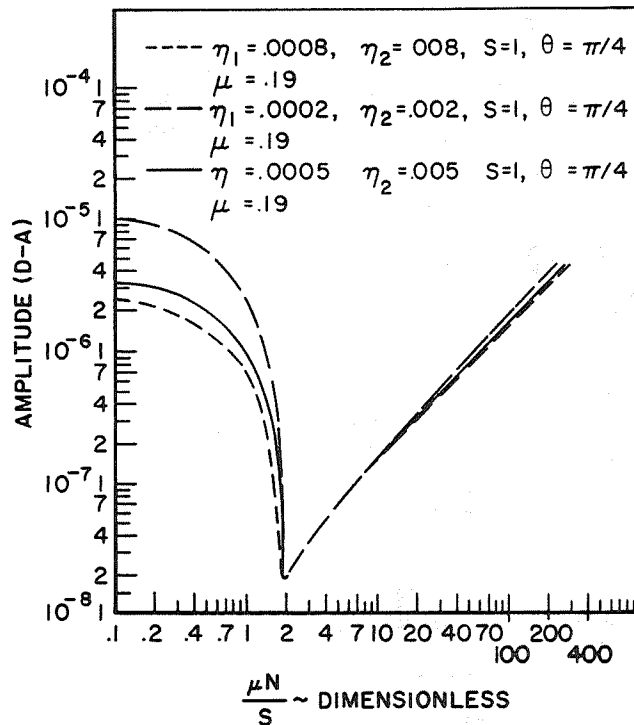


FIG. 7 AMPLITUDE OF m_1 RELATIVE TO m_2 VS $\frac{\mu N}{S}$,
VARIATION OF η_1 η_2

order (E) of vibration $n/2$, produces a higher level of Coulomb friction damping, as expected. However, this is not usually a controllable parameter in an operational turbine, as may be true of most of the other parameters. The figure does show the characteristics of the curves for various engine orders of excitation, and provides useful design or evaluation information. It should be noted that the amplitude reduction possible is the same for all values of θ but at different values of $\mu N/S$.

Figure 9 shows the effect of variation of S , the forcing function amplitude. It should be noted that the three curves shown have identical shapes, but that for an order of magnitude increase in S the airfoil response amplitude (D-A) as a function of $\mu N/S$ increases by an order of magnitude. This shows the

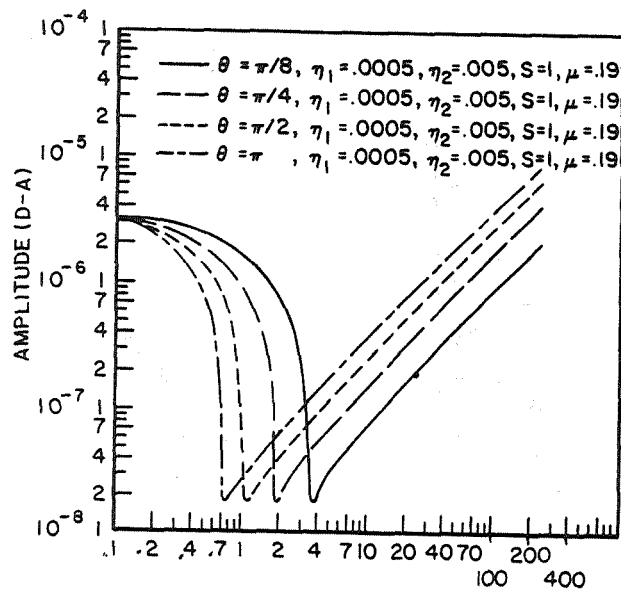


FIG. 8 AMPLITUDE OF m_1 RELATIVE TO m_2 VS $\frac{\mu N}{S}$,
VARIATION OF θ

system to be linear with S and indicates that a unit curve ($S=1$) can be used to define a system. Then, the response amplitude can be scaled by the amplitude of S for any operating system having otherwise identical operating parameters.

All the previous data sets represent systems having a μ (the damper to platform coefficient of friction) of 0.19, an arbitrary value. A set of data was generated for a system having μ of 0.38, double the previous value. When a data point for $\mu N/S$ of $\frac{0.38 \times 5}{1}$ was plotted, the amplitude fell identically on that for $\frac{0.19 \times 10}{1}$, and similarly for all values of $0.19 \times N$ equivalent to $0.38 \times N$. Obviously μ and N are not independent variables, which is a basic tenet of Coulomb friction. It is necessary to know the values of μ and N and their characteristics throughout the operating temperature-pressure-speed regime of a turbine. They may be amenable to some modification if design problems are encountered, or if operational fatigue problems are

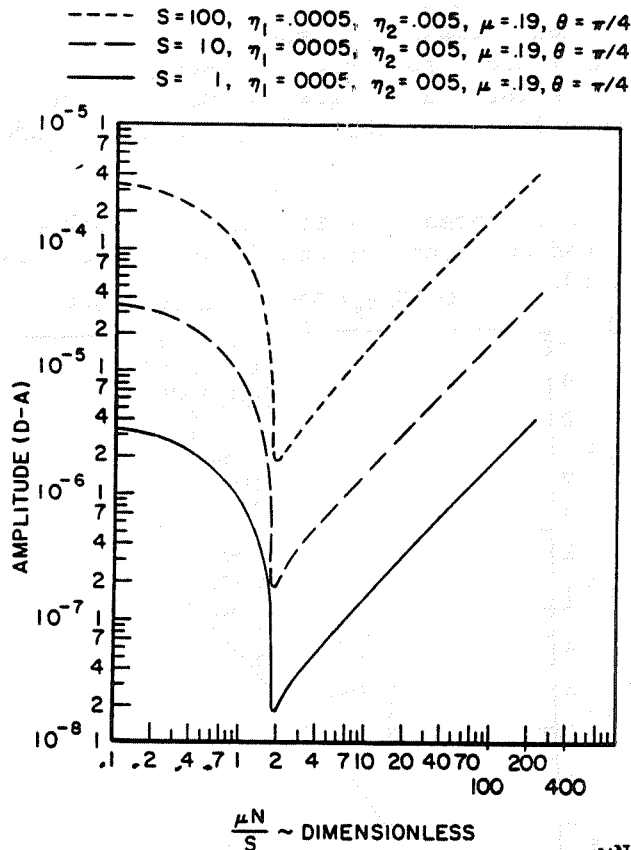


FIG. 9 AMPLITUDE OF m_1 RELATIVE TO m_2 VS $\frac{\mu N}{S}$,
 VARIATION OF S

encountered later that necessitate modification of the system.

A limit of this dynamic analysis is that the Coulomb friction ends at some value of $\mu N/S$ and a regime of stick-slip friction begins. The stick-slip regime is followed by the end of slip, the lockup regime where friction ends and the surfaces are locked firmly together. The consequence of platform lockup has been shown to be quite severe for the system under study, being almost immediate failure of the turbine blade. After the loss of friction damping the airfoil vibration amplitude at excited resonance modes is limited only by the blade material hysteretic loss

factor (perhaps 0.0001) combined with whatever aerodynamic viscous damping is imparted to the blade by the driving fluid. For this analysis the outboard blade section loss factor was estimated to be an order of magnitude less than that of the inboard blade section.

The consequences of stick-slip and lockup have been sketched on a copy of the Figure 6 graph as shown in Figure 10.

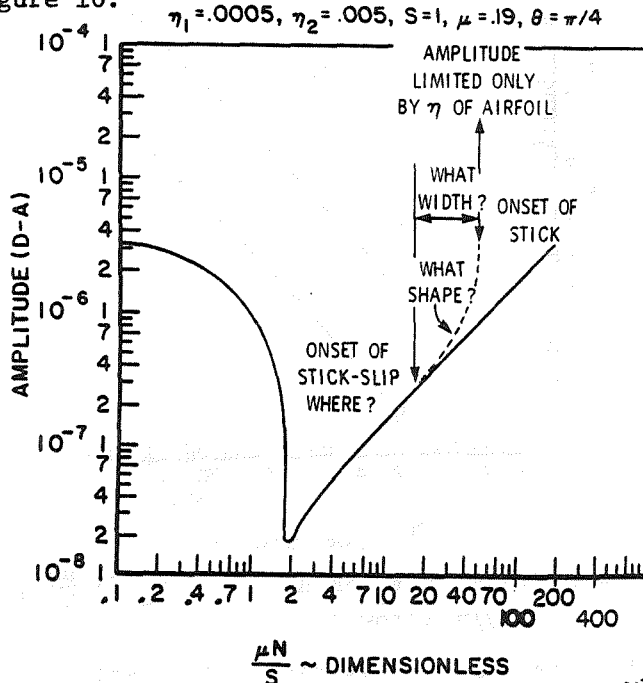


FIG. 10 AMPLITUDE OF m_1 RELATIVE TO m_2 VS $\frac{\mu N}{S}$,

EFFECTS OF STICK-SLIP AND STICK

The location of stick-slip onset, the breadth of the stick-slip range and the effective damping in that range may be critical to system survival. This information is likely to be indeterminate without a careful and costly test program. Such a program may yield only marginally satisfactory results. What is needed is instrumentation data readings during system operation. Acquisition of such data is still beyond the state of the art for some high performance systems

such as the HPFTP.

The following conclusions are drawn from this study.

1. The lumped mass analysis shows the qualitative effects of the platform friction dampers on the flexural resonance response modes of the subject blade in the frequency range of 0 to 20,000 Hz.
2. Good quantitative analysis is dependent on reliable knowledge of the parameters upon which the analysis is based, i.e., m_1 , m_2 , k_1 , k_2 , η_1 , η_2 , μ , N , S and θ or δ , these latter being functions of the engine order of the excitation and the number of blades in the disc.
3. The analysis shows that effective friction damping is achieved in the lower range of the parameter $\mu N/S$ up to the value where $\mu N/S$ causes the onset of stick-slip friction. The airfoil amplitude response during stick-slip is undefined and if stick is encountered the airfoil amplitude will be controlled only by the damping of the airfoil section of the blade.
4. The response amplitude of the airfoil is reduced more than two orders of magnitude (more than 99 percent) at the minimum response in the frequency transition region ($\mu N/S$ range approximately 1 to 10, dependent on θ).
5. The hysteretic damping of the blade does not appreciably affect its response in the effective friction damping range.
6. The curves shown in Figures 7 through 9 define the effects of variations of η , θ , and S in the $\mu N/S$ region where stick-slip and stick are not encountered.
7. Figure 9 shows that response curves for $S=1$ can be used for design or redesign of this blade-damper system since the response amplitude scales linearly as a function of S .

8. The values of $\mu N/S$ that cause onset of stick-slip and stick are critical to the damper system design. If these regions can be avoided the Coulomb friction damping is very effective.

Test Evaluation in the Spin Pit

A vibration test evaluation of a simulated HPFTP first stage bladed disk was conducted in a high speed spin pit. For purposes of test, a used set of blades and dampers was acquired from NASA and a titanium disk and two types of experimental dampers were fabricated. Blade vibration responses were measured with strain gages as the blades were excited magnetically during high speed spins in vacuum.

Twelve blades were instrumented with 1/16 inch square strain gages on the suction side of the airfoil. The gages were centered 1/4 inch above the platform and 1/8 inch from the trailing edge, a high stress region of the blade. Leadwires were routed down the aft face of the blade through a slot cut in the platform to terminals on the aft face of the firtree area. A photograph of a strain gage installation is shown in Figure 11.

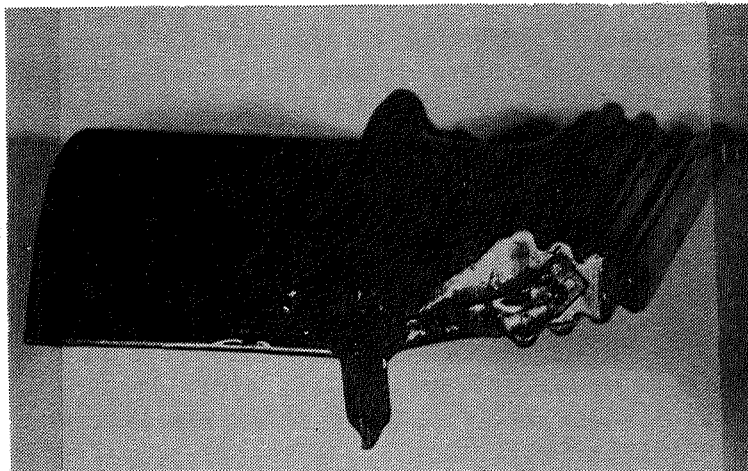


FIG. 11 HPFTP STRAIN GAGED BLADE

The blades were installed in a test disk .

fabricated from a forged and heat-treated 6Al4V titanium blank. The firtree slots in the disk were cut by computer controlled wire EDM, which achieved production tolerance on the slot configuration and the blade to disk firtree fit. The test disk was fabricated with 64 slots in order that a symmetrical test specimen could be assembled.

In addition to the disk, two types of lightweight experimental platform friction dampers were fabricated. These dampers were formed of nichrome wire on bending jigs designed for the purpose. Figure 12 shows the production 0.56 gram dampers and the experimental 0.20 gram and 0.10 gram dampers.

After 0.5 gram magnetic cobalt weld beads were added to the blade tips, the blades were tested in a broach block to identify the first flexural and first torsional mode resonance frequencies. They were subsequently x-rayed to verify the adequacy of the welds and the absence of serious cracks. They then were weighed and were installed in the test disk in the scheme shown in Figure 13. As shown, eight groups of

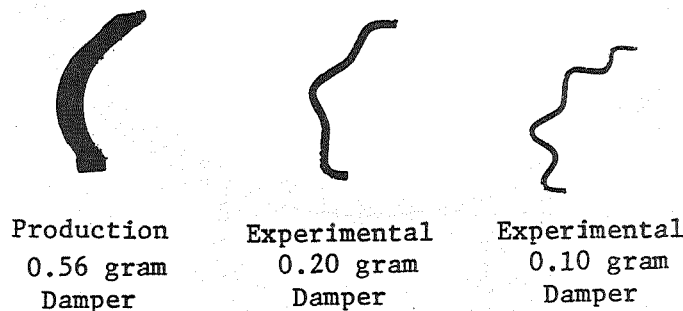


FIG. 12 TEST DAMPERS

eight blades were installed in test octants consisting of oppositely balanced octants of each of the three test damper types and two opposite groups of blades without dampers. Two strain gaged blades and one spare gaged blade were included for each configuration type. In addition, two gages were installed to measure radial strain on the test disk. The blade strain gages were connected to leadwire pairs on the disk with

amplifiers and on to an FM reorder and to test monitoring oscilloscopes and a frequency analyzer.

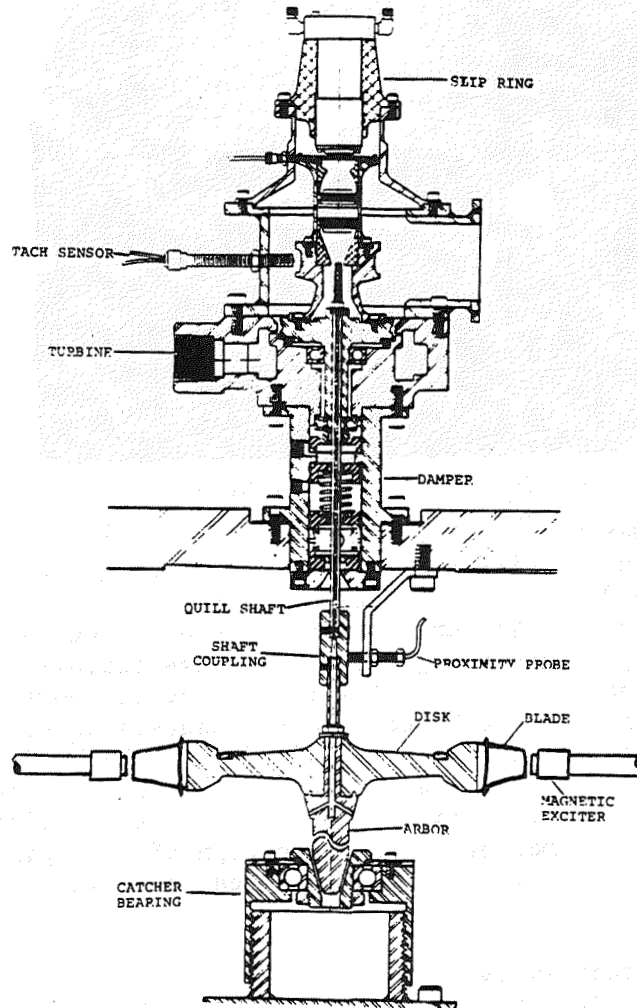


FIG. 14 SPIN TEST ASSEMBLY

As shown in Figure 14, the blades were excited by radially mounted samarium cobalt permanent magnets that were spaced symmetrically around the disk with an at-rest gap of 0.12 inch between the magnets and the cobalt weld beads on the blade tips. The magnet support

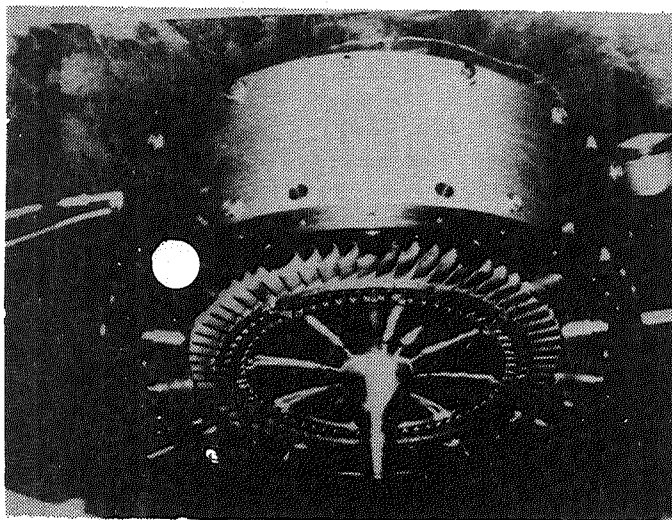


FIG. 15 SPIN TEST SET-UP

fixture was provided with 28 magnet mounts and tests were conducted with both 28 and 14 magnets installed, providing 28E or 14E excitation of the bladed disk for two series of test runs. Whether 28 or 14 magnets were installed, adjacent magnets were always installed with opposite polarity, i.e. if a magnet had its north magnet pole facing the blade tips the magnets on either side had their south magnet pole facing the blade tips. The blades were excited primarily by magnetic drag pulses as the blade tips passed through the fields of the permanent magnets. A photograph of the spin pit test setup with 14 magnets installed is shown in Figure 15.

The test assembly was always spun in a vacuum that ranged from 2.5 to 3.0 torr for various test spins. In early testing, high whirl modes of the test assembly were encountered but these were reduced to tolerable levels by redesigning the arbor to quill shaft coupling. The first spin test was conducted with 28 excitation magnets installed. It was expected that this 28E excitation would induce the first flexural resonance mode of the blades (4,800 Hz was the mean frequency for 64 blades hard clamped in the broach block) at about 10,000 rpm and that the 8,500 Hz airfoil-alone first flexural mode might occur near 18,000 rpm, at least on

the blades with the heaviest (production 0.56 gram) dampers since frequency increases linearly with rpm and normal force of the dampers increases with the square of the rpm.

The first test spin covered the range from 0 to 23,000 rpm. The only significant test data from this spin are shown in Figures 16, 17, 18 and 19.

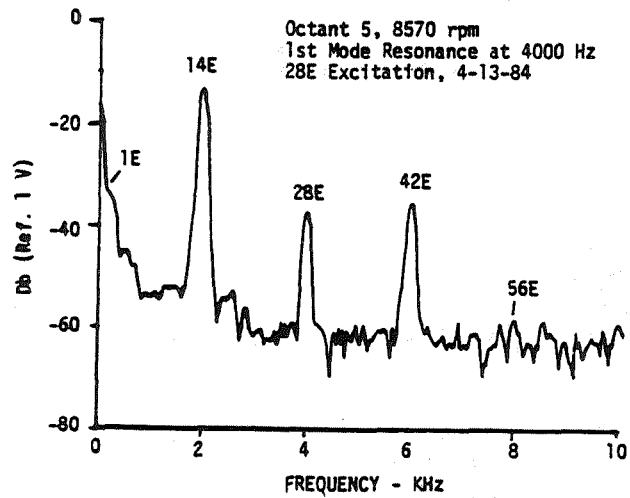
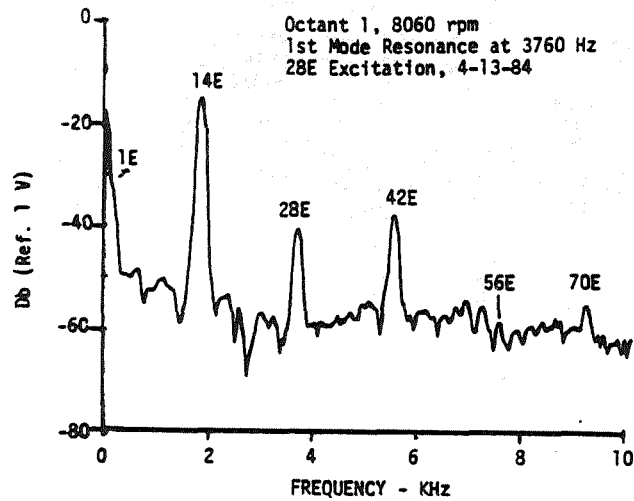


FIG. 16 VIBRATION SPECTRA - UNDAMPED BLADES

First flexural resonance vibration of all the monitored test blades is shown clearly at the 28E excitation frequency. The peaks at 14E and 42E are due to magnetically induced EMF in the strain circuits and the 1E peak is due to one-per-rev unbalance-induced strain. The signal noise floor is caused by sum and difference frequencies of the one-per-rev signal and its harmonics with the other major signal components.

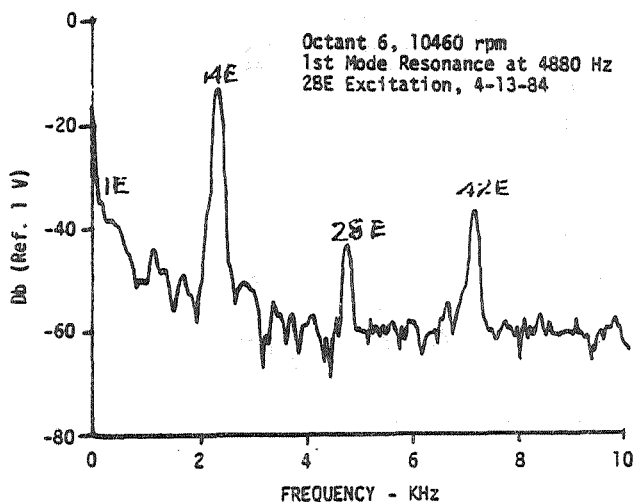
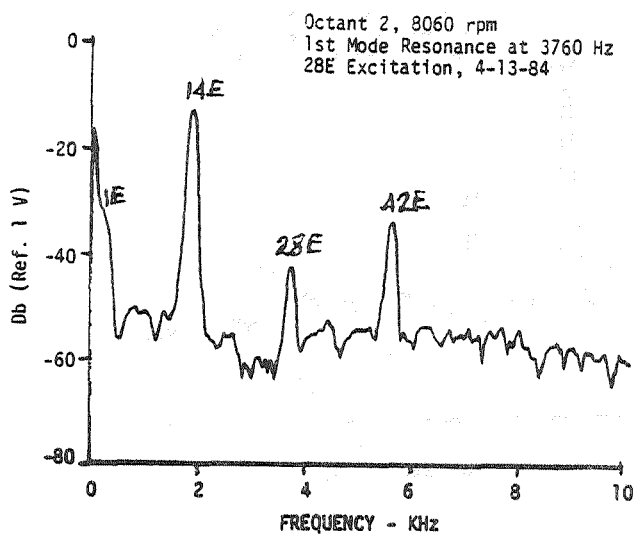


FIG. 17 VIBRATION SPECTRA-PRODUCTION 0.56 GRAM DAMPERS

By contrast, Figure 20 shows strain gage signals for 28E and 14E excitation spins when no blade resonance vibration is occurring.

The significant factors shown by the low speed spin data of Figures 16 through 19 are that the blade first flexural mode resonance occurred at lower than expected

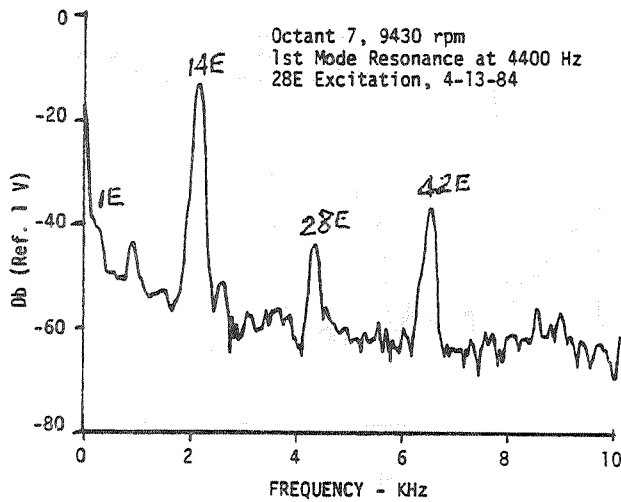
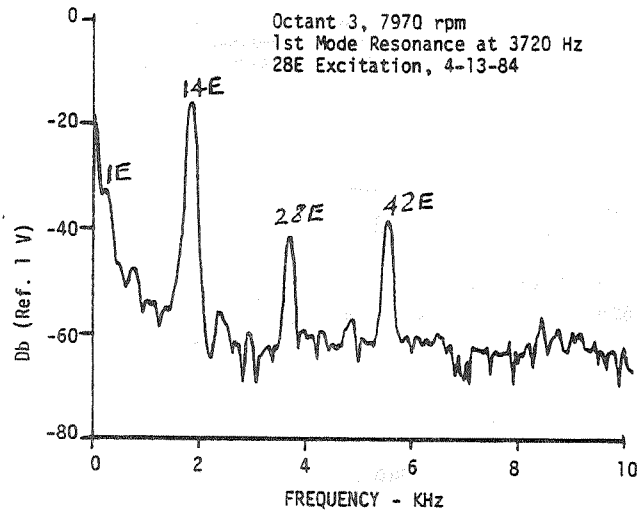


FIG. 18 VIBRATION SPECTRA - EXPERIMENTAL
0.10 GRAM DAMPERS

frequencies for all four test configurations and that no airfoil-alone resonances occurred for any of the instrumented blades. The first torsional mode resonance was found for two blades near 10,700 Hz and 23,000 rpm, but at a relatively low amplitude. The surprisingly low first flexural mode frequencies found during this spin test are attributed to a relatively

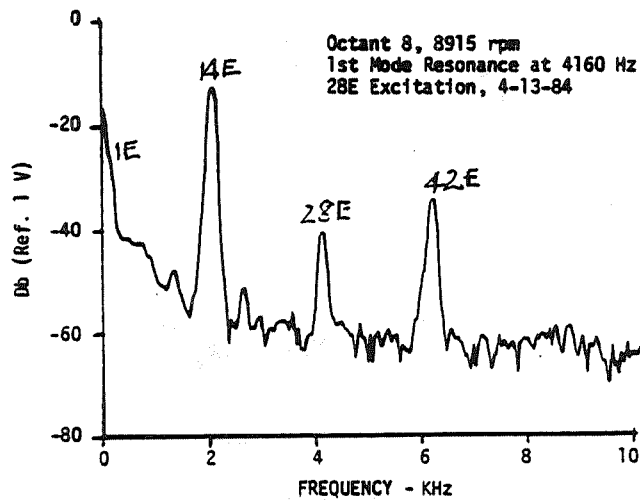
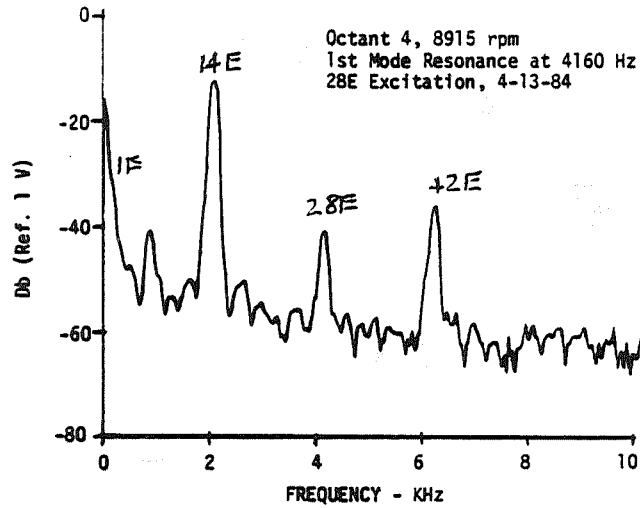


FIG. 19 VIBRATION SPECTRA - EXPERIMENTAL
0.20 GRAM DAMPERS

soft mount condition of the blades at the firtree root for this low speed spin condition.

After the magnets were reconfigured for 14E excitation, a high speed spin test to 38,000 rpm was performed. The only significant blade resonance vibrations found during this test are shown in Figures 21 and 22. Figure 21 shows the first flexural mode

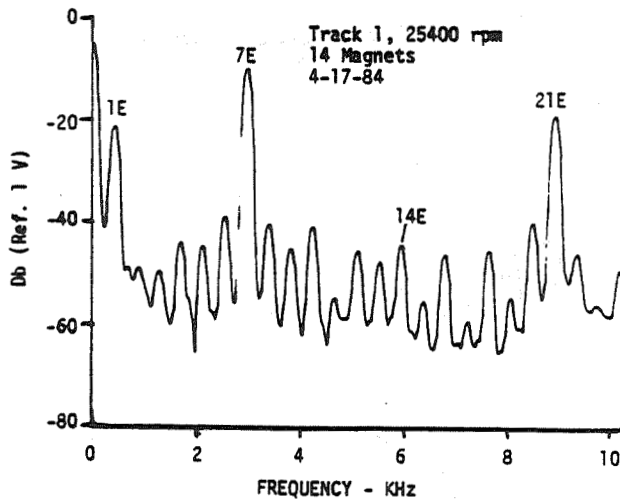
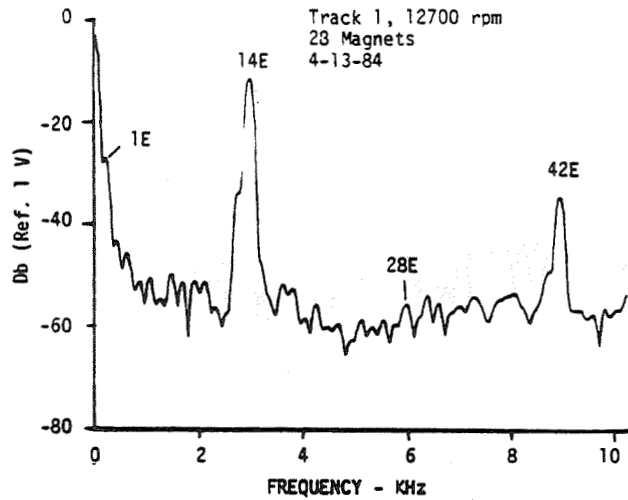


FIG. 20 OCTANT 1 FREQUENCY SPECTRA - NO RESONANCE

vibration of the whole blade for the blades with no friction dampers and Figure 22 shows the airfoil-alone flexural resonance mode for blades with production 0.56 gram dampers. Neither mode was found for the blades with lightweight experimental dampers indicating vibrations of these blades occurred at very low amplitude in the transitional region between the two resonance

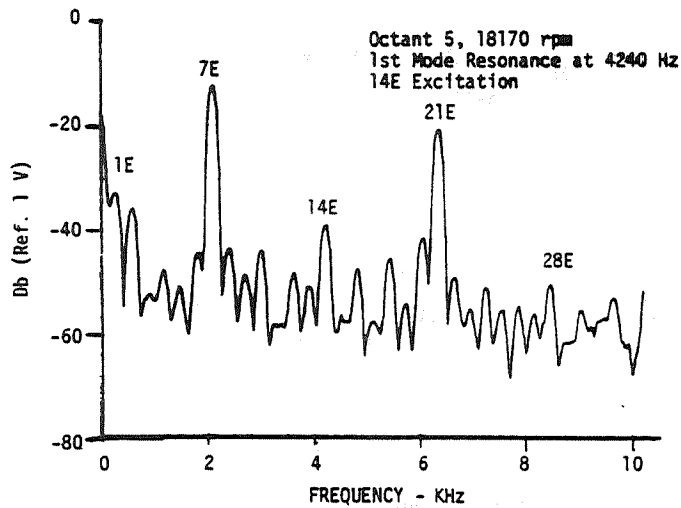
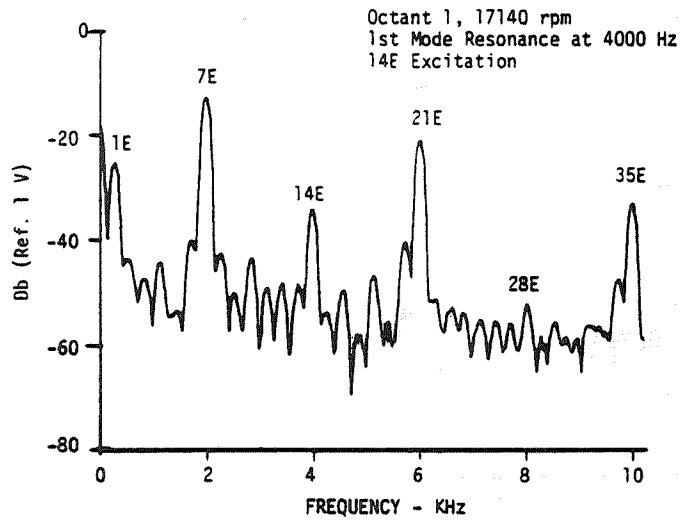


FIG. 21 VIBRATION SPECTRA - 14E EXCITATION OF UNDAMPED BLADES

modes. In other words, these friction dampers worked very well at the excitation force levels produced by the permanent magnets. Conversely, the production 0.56 gram dampers caused an airfoil-alone resonance vibration strain signal in test octant 6 that was more than 6 dB higher, or double the strain amplitude, than any of the resonance vibrations that occurred in the

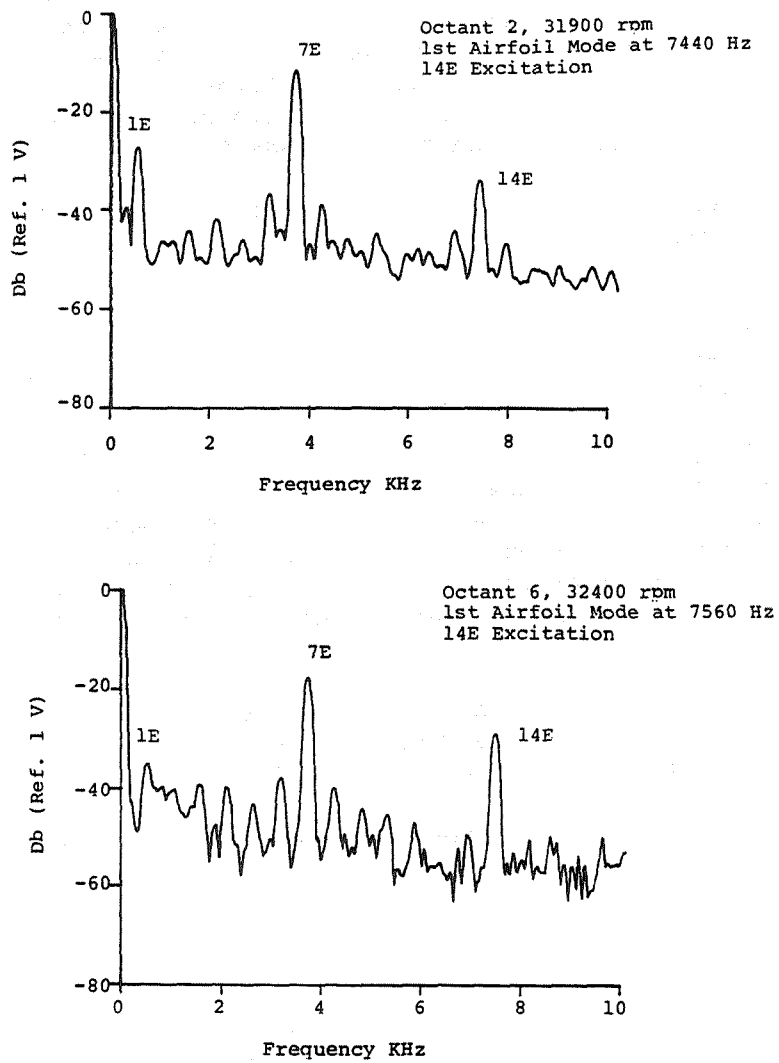


FIG. 22 VIBRATION SPECTRA - AIRFOIL FLEX MODE -
PRODUCTION 0.56 GRAM DAMPERS

undamped blades or in any of the blades in the whole blade first flexural resonance mode.

The resonance vibrations shown for undamped blades in Figure 21 again occurred at a lower than expected frequency but at a higher frequency than in the low speed spin test. This shows a relatively soft, but hardening, root fixity at the firtree. The airfoil-alone flexural resonance modes shown in Figure 22 also occurred at a lower than expected frequency. This is attributed to the addition of the 0.5 gram magnetic cobalt weld beads added to the blade tips.

The following conclusions are drawn from the test program.

1. Low speed spin conditions are not adequate to seat the blades and dampers firmly enough to produce data related to conditions during operational speeds of the HPFTP.
2. The production 0.56 gram dampers did constrain the platforms at operational spin speed and caused excessive airfoil-alone first flexural mode resonance vibration, though probably at a lower than operational excitation amplitude, at the 14E excitation frequency that is known to occur in the HPFTP.
3. Lightweight experimental dampers eliminated both lower order flexural modes of the blade for the excitation level that occurred in the test.
4. The test data confirmed the results of the analytical study.

Acknowledgement

This work was performed for Marshall Space Flight Center (MSFC) of NASA under contract NAS8-34682. Mr. Larry Kiefling, the project technical monitor, of the Structural Dynamics Division of MSFC, was very helpful in providing data and guidance for the work.

References

1. Muszynska, A., D.I.G. Jones, T. Lagnese, and L. Whitford, "On Nonlinear Response of Multiple Blade Systems," Paper presented at 51st Shock and Vibration Symposium, San Diego, CA, October 1980, and published in Shock and Vibration Bulletin 51, Part 3, May 1981.
2. Sutton, R.F., "Nasa, High Speed Rotating Diagnostic Laboratory Testing, SSME High-pressure Fuel Turbopump Blade/Damper Evaluation," Rocketdyne Division of Rockwell International Report RSS-8626, November 2978.
3. Dominic, R.J., "Parametric Study of Turbine Blade Platform Friction Damping Using the Lumped Parameter Analysis," ASME Paper 84-GT-109, 1984.
4. Dickerson, E.O., "Turbine Blade Structural Dynamic Analysis," AIAA Paper 80-0782, 1980.
5. Scott, L.P., J.E. Pond, C.C. Myers, G.A. Teal, G.F. Lewis, and J.K. Robinson, "Assessment of HPFTP Turbine Blade Environment and Fatigue Life Study on the SSME, Volumes I and II," Lockheed Missiles and Space Company, Inc., Huntsville Research and Engineering Center Report LMSC-HREC TR D784198, May 1981.
6. Dominic, R.J., Philip A. Graf, and B. Basava Raju, "Analytical and Experimental Investigation of Turbine Blade Damping - Final Report," University of Dayton Research Institute Report UDR-TR-82-39, August 1982. (AD-A120470, AFOSR-82-0911TR, or NTIS HC A04/MF A01).
7. Soni, J.L., and T.W. Held, "Users Manual for a Computer Program for Dynamic Response of Bladed Systems," University of Dayton Research Institute Report UDR-TR-84-38, May 1984.